Application of FEA to Image-based Models of Electrical Trees with Uniform Conductivity

Simon M. Rowland[1], **Roger Schurch**[1,2], **Michalis Pattouras**[1] and **Qi Li**[1]
[1]School of Electrical and Electronic Engineering, University of Manchester, Manchester, UK
[2]Department of Electrical Engineering, Federico Santa Maria Technical University, Valparaiso, Chile

ABSTRACT

X-ray computed tomography and serial block-face SEM have provided detailed three-dimensional reconstructions of electrical trees for the first time. The application of finite element analysis (FEA) to the analysis of electrical fields in an epoxy block containing a tree is considered. Illustrations are provided by way of a number of case studies. It is shown that the limitations of FEA do not arise from the discrete nature of the meshing: rather uncertainties are more concerned with material properties in high fields on the micrometer scale, the limitations imposed by the pixel size of the imaging technique, and the discrete nature of the image reconstruction technique. For a dynamic model of tree growth space charge dynamics on the same physical scale need also to be modelled. A meshing strategy is used, calibrated against the charge simulation method, to ensure accurate but manageable computations in critical parts of a tree such as branch tips. Examples of field values are given using geometric constructs and low-field material characteristics as illustrative values. The field variation around a conducting tree structure, including the maximum field direction as a branch starts to bifurcate, is determined as an example. These yield values in excess of those expected if space charge movement was considered, but consistent with analytical calculations.

Index Terms - **XCT, x-ray computed tomography, SBFSEM, Serial block-face SEM, FEA, finite element analysis, electrical tree, field, model, charge simulation method, CSM, image-based modeling.**

1 INTRODUCTION

ELECTRICAL trees are the result of long-term ageing mechanisms in polymeric materials and can lead to failures in high voltage equipment. Such trees normally originate in locations where voids, impurities and/or protrusions cause a high, divergent electric field. During periods of growth, partial discharges are observed, and growth is widely considered to be a result of these discharges. Sixty years ago Mason showed, for example, that pitting resulted from discharges within channels in polyethylene, and identified that carbonization of surfaces occurred in some cases and not in others [1]. Under high AC voltages, the discharges in the voids eroded their surface creating non-conducting protrusions into the material. As the discharges continued, the protrusions became conductive locally enhancing the electric field and subsequently resulting in the growth of a tree.

Much of what is understood concerning tree growth has been learnt from direct observations of laboratory grown trees in transparent polymers. Direct optical measurements of the visual aspect of trees, and associated partial discharges and optical emissions [2, 3] have become standard in their study.

Manuscript received on 8 September2014, in final form 7 January 2015, accepted 8 January 2015.

In most laboratory experiments, electrical trees are grown in pure polymer resins using needle-plane geometries to create very high divergent fields, but in service trees grow in apparently less onerous conditions over longer times [4]. The use of needle-plane geometries enables high fields to be achieved at relatively low voltages, and easy observation of the tree growth in the transparent materials. Such trees are observed to grow from a length of 10 μm to cross the insulation, typically a few mm, before total breakdown occurs. Electrical trees are typically classified as one of three types: branch, bush, or bush-branch depending on their apparent similarity with botanical tree shapes [5].

Laboratory-grown trees are normally observed by optical microscopy. This results in a two-dimensional (2D) projection. The depth of field of the projection depends upon the microscopy system used, and this influences the image, as seen in Figure 1. Each 2D projection of a tree can be characterized by a fractal dimension, f_d [6]. Kudo pointed to the limitations of fractal analysis of a three dimensional (3D) object with a 2D image [7]. Typically values determined from such images are $1 < f_d < 2$ for branched and $2 < f_d < 3$ for bush trees [8]. The tree shape and characteristics are heavily dependent on the voltage (field) applied, the material (composition and glass transition temperature) and mechanical stresses [9]-[12].

Scanning electron microscopy (SEM) and Transmission electron microscopy (TEM) [13] have given excellent

DOI 10.1109/TDEI.2015.004922

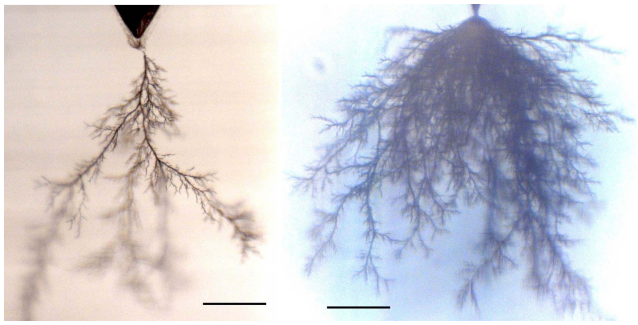

Figure 1. A branched (left) and a bush type tree (right) created in laboratory conditions. Scale bar: 200 µm.

localized images of individual tree branches / tubules. This has provided direct evidence of the physical nature of such features: confirmed to be connected tubes of diameters of the order of microns. Figure 2 reproduces two excellent images taken by SEM of a tree grown in polyethylene, after microtoming and etching. However the potential for developing a full understanding of the three-dimensional structure of the trees from this approach is limited.

Recent research has allowed complete three dimension (3D) replicas of trees to be generated using both X-ray computed tomography (XCT) and serial block-face scanning electron microscopy (SBSEM) [15, 16]. The use of these methods enables the measurement and calculation of many quantities which characterize the tree: for example, parameters such as the diameter of tree channels, tree volume and surface area, and 3D fractal dimension [17]. Also, parameters from the skeleton of the tree can be obtained: number of vertices and segments, segment lengths, branch angles and tortuosity of the channels, amongst others.

Moreover, the reconstructed 3D models may, for the first time, allow field estimations to be made in the dielectric containing a tree, in particular using FEA. However, this begs the question of what FEA is capable of at such scales, and also what the true nature of a tree is and how that can represented by the 3D model. This paper addresses these questions, not to generate a new model of tree growth at this stage, but to determine whether FEA is an appropriate tool with which to build field models. As a starting point: a time independent, discharge-free model will be considered.

In the following section the reconstructed trees are introduced. This is followed by considerations of the physical parameters used to generate the FEA structure. Finally the models are generated and their limitations considered in detail.

2 GEOMETRIC THREE-DIMENSIONAL TREE RECONSTRUCTION

Three-dimensional models (or 'virtual replicas') from 'real' (rather than simulated) electrical trees have been generated using the imaging techniques of X-ray computed tomography (XCT) and serial block-face scanning electron microscopy (SBFSEM) [15, 16]. In the past, optical microscopy combined with either computed tomography or serial sectioning methods were used to reconstruct the structure of trees [17]. However, optical tomography cannot resolve complex trees and

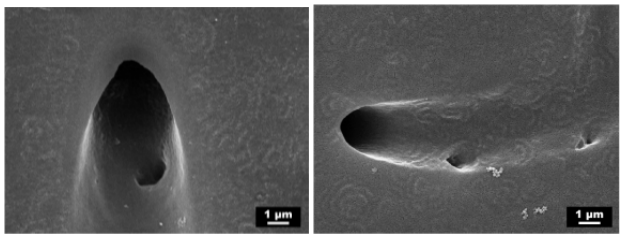

Figure 2. SEM images of microtomed surfaces giving cross-sections of tree branches [14].

optical microscopy is limited in resolution. In contrast, XCT and SBFSEM can provide sub-micrometer resolution and be applied to optically-opaque materials [18]. The general methodology for electrical tree 3D model creation consists in experimental sample preparation, electrical tree formation, machining the sample to prepare it for the scan, image acquisition and post-processing of the data which includes image segmentation and surface generation.

XCT is a non-destructive technique based on the measurement of transmission of X-rays through an object over a range of angles. A series of radiographic projections are taken as the sample is rotated axially and then combined with a reconstruction algorithm to form cross-sectional images ('slices') of the volume [19]. In conventional X-ray imaging, contrast is obtained from the attenuation of X-rays as they pass through the object. However, when imaging electrical trees in polymers, attenuation (absorption) contrast does not provide sufficient contrast between the material and the gas filled tubes comprising the tree. As an alternative, contrast can be obtained from the phase shift in the X-rays as they pass through the object. This mode is called 'phase-contrast' and has been shown by the authors to be well-suited to electrical tree imaging [16]. In this mode, the distortion of X-ray wave-fronts (phase shift of the X-ray waves) is due to the different refractive indices of the different materials present in the object thus, phase contrast can be observed even when absorption contrast is almost undetectable [20].

In SBFSEM, the 3D set of data is acquired by automated serial sectioning combined with block-face imaging of the sample, inside a chamber of a low-vacuum SEM [21]. By maintaining a gaseous environment around the sample, this technique allows SEM imaging of non-conducting surfaces, removing the need for a conducting coating and thus, enabling automated serial sectioning inside the chamber.

The final output from both imaging techniques is a stack of images (slices) that represent cross-sections of the electrical tree (a selected slice is shown in Figure 3a). These slices are in grey levels, where different pixel intensities represent different materials (XCT and SBFSEM) or surface topological information (SBFSEM only). From this stage, the model creation procedure follows the same route in both imaging techniques. The pixel size of the images relates to the resolution of the scan and the dimensions to the field of view captured. Using the gray level information, the procedure follows to image segmentation, which is the process whereby the feature (electrical tree) is extracted and labelled. In this process, a new stack of images is generated, where pixels are no longer gray scale levels but color-labelled (8 bit depth).

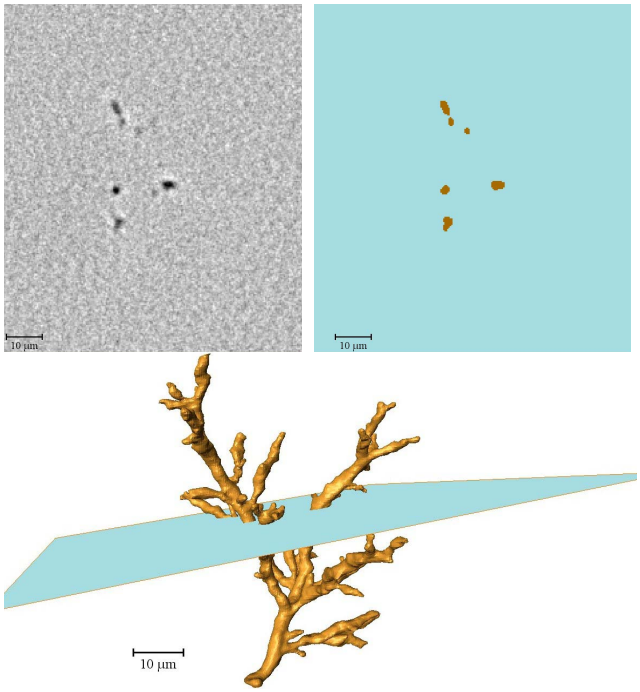

Figure 3. a) Cross-sectional slice in gray levels obtained from reconstructed XCT scan; **b**) Slice after segmentation process; c) Model generated and the location of the slice shown in a) and b). All scale bars: 10 µm.

Each color represents a different material. In the case of electrical trees in unfilled epoxy, images are composed of only two colors: electrical tree and epoxy resin (see the selected segmented slice in Figure 3b). With these segmented slices, numerical quantification and surface generation (3D model or virtual replica) is possible. The generation of the surface of the electrical tree (a closed volume) involves connecting the labelled pixels among the slices and computing a triangular approximation of the interfaces between different materials. This process was carried out using Avizo software, where different smoothing types and extent levels are available. Surface smoothing is required in order to avoid artificial 'staircase-like' surfaces resulting from the connection of voxels (3D pixels), but without modifying the original shape of the feature. Despite special care, this smoothing process may modify details of the tree or create artificial features. For the case presented here, the lowest smoothing extent that removed the staircase-like nature of the model surface was chosen. An example of the surface generated is shown in Figure 3c.

Many elements may hinder the generation of the best possible (closest to reality) 3D model: First, issues relating to image quality of the slices from the scans. Image quality is affected by resolution, contrast, noise and artefacts [22]. Currently, the final spatial resolution using these 3D imaging techniques is around 0.7 µm for XCT and in the case of SBFSEM, in practice around 0.1 µm [16]. The second hindrance can be misguided decisions about which gray levels represent tree tubes during the image segmentation process. As discussed earlier, in reality there is unlikely to be a clearly defined surface at the sub-micron scale. Finally, surface generation from the segmented slices requires decisions about the level of surface smoothing. This greatly affects the model for FEA use, through the inclusion or exclusion of sharp points or singularities. Among the factors that affect the accuracy of the model generated for FEA, the ones that are most influential are: the image quality of the slices (mainly resolution) and surface generation (selection of smoothness and subsequent inclusion of singularities).

In the exercise of creating virtual replicas of electrical trees to be used in FEA modelling, it is worth asking not only what the inaccuracies of generating 3D models from the scans are, but also, what is missing from the imaging scans. It is not really known what features are not seen (this is also true for optical techniques). Any tube finer than the spatial resolution of the images, will not be captured.

The data used for the 3D model shown in Figure 3 was acquired using XCT and a pixel size of 0.37 µm. The 3D model generated has the following characteristics [23]: a length of 59 µm, tree channel diameters of around 2 µm, a tree volume of 1.6×10^3 µm^3, a tree surface area of 3.5×10^3 µm^2 and a 3D fractal dimension (box counting method) of 1.7. The characteristics of the skeleton of the tree were: 78 vertices, segment lengths of around 7 µm, branch angles averaging 67° and tortuosity of tree channels of 1.2.

3 MODEL PARAMETERS

So that a model can be constructed, assumptions concerning the physical nature of the tree need to be explicitly considered. Reviewing the literature, this is now considered in three parts; the gaseous phase (within the tubules), the interface between gas and polymer, and the bulk polymer.

3.1 THE GAS PHASE

In a passive tree in which no discharges are active the gas will have a similar constitution to air perhaps with some volatiles from the surrounding polymer, and at atmospheric pressure. During periods in which partial discharges are occurring the gas will be partly ionized - more so at the discharge time and location, and less elsewhere. In addition, volatile by-products from the polymer surface are likely to be present. Pressure is likely to fluctuate as gaseous constituents are consumed or generated through consumption of oxygen initially and the low molecular weight species being volatilized from the tree wall surface [24, 25]. During and after partial discharge evolution, a change in ionic density and air conductivity will also occur.

It is clear then that for a complete model of behavior the time dependent properties of discharges, and their interaction with the polymer surface becomes important. This is not considered here, and the channels are considered to be air-filled with a fixed, uniform conductivity.

3.2 THE INTERFACE BETWEEN GAS AND POLYMER

Electrical tree conductivity plays an important role towards the shape and propagation of the tree, and as such their classification as 'conducting' or 'non-conducting' has become normal practice. By 'conducting' is normally meant that the interface between the gas and dielectric solid phase is conducting and it is normally associated with a carbonaceous layer. Vaughan et al found the difference between areas of tree

with and without carbon to be quite distinct [26]. The simplest considerations of this are that if the tree is conducting, the field within is negligible and so discharges will not occur in its branches, but the field at the branch tips will be enhanced and so discharges will preferentially occur there. The ability or otherwise of a tree to sustain a discharge within its extent is considered to be one reason for it to grow as a bush- or branch-type: conductive tubules generally being considered to prevent internal discharges, and so lead to branch-type trees [27]. It has also been speculated that a change in conductivity along a tree may also be associated with a branch point [5]. Values of tubule conductivity for conductive trees were estimated at between 1–10 Ω/μm in polyethylene by Vaughan [28] using a resisitivity of 10^{-3} Ωcm and a wall thickness of 0.5 µm. Values of 1×10^{8} and 1×10^{12} Ω/50µm were respectively modelled as producing conducting and non-conducting trees respectively by Champion and Dodd [27].

3.3 THE BULK POLYMER

It is likely that the polymer in which the tree grows has time-varying properties, particularly in regions of tree growth and high fields [29]. The mobility of charge carriers will vary between polymers, and will also be a strong function of temperature, particularly around the glass transition temperature. The highly divergent field expected at the needle point and tree tips is likely to create a large variation in electrical conductivity. It has long been accepted that space charge injection at the high fields generated will modify and moderate the fields otherwise expected [30]. In the case considered here it is assumed that no space charge enters the polymer, and that the bulk polymer is uniform. Therefore the fields calculated in these models do not represent expected values: but enable exploration of the process of evaluation and spatial resolution using FEA and the imaging techniques. In the epoxy resin case considered, the following values have been taken: relative permittivity $\varepsilon_r = 3.6$, and conductivity $\sigma = 1\text{x}10^{-13}$ Sm^{-1}.

4 FEA MODELS

In general, the Finite Element Method can be divided into five procedures:

- determining the geometry of the model
- meshing
- assigning boundary conditions
- solving
- post process and results analysis

Due to the complexity of the electrical tree, specific techniques are required within each step to achieve high accuracy in field calculations. These are now considered.

4.1 GEOMETRY MODELING

The electrical tree geometrical model is generated using Avizo software as explained in Section 2 and includes the host epoxy cube of 20 mm sides. The simulation is concerned with the electric field distribution within the cube only. Figure 4 illustrates the tree geometry explored.

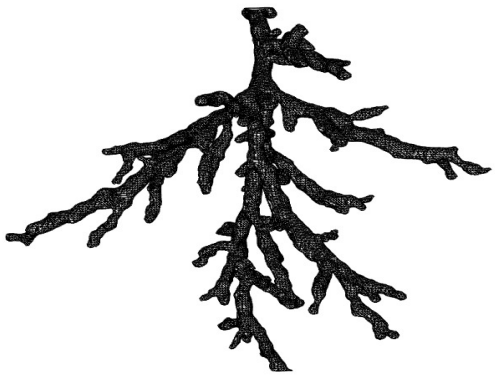

Figure 4. The imported XCT geometry for modelling in FEA. The tree is 59 µm long.

4.2 MESHING TECHNIQUE

The model deployed for simulation has relatively fine details (tree branches) within a large simulation domain (the epoxy cube). One challenge of performing such a simulation is forming a proper strategy for mesh generation. An appropriate meshing scheme is critical for the successful simulation of the in terms of accuracy, given the computing resource available.

The scale factor (μ) is defined as:

$$\mu = \frac{l_{\max}}{l_{\min}} \tag{1}$$

where $l_{\max}$ and $l_{\min}$ refer to the maximum and minimum length of a feature within the whole simulation. The minimum edge length within the geometry is set by the sharpest tip of electrical tree branches which has a diameter of 0.2 µm while the maximum size is the edge of the epoxy cube of 20 mm. This creates a scale factor of 100,000 and requires a large computing memory in order to obtain an accurate result.

Figure 5 illustrates the process of adaptive mesh refinement. To apply it to the electrical tree model, a preliminary solution is computed first. This tentative model assumes a conductive tree (the potential of the tree channel is the same as the voltage applied on the needle). The electrostatic equations are applied to this model. Within this step of study, the mesh is not optimized and a coarse mesh is generated to sketch the field distribution. The local maxima are determined by analyzing the volume electric field distribution.

As expected, the local maxima are located at the tips of the tree branches in the solid dielectric. This is due to the divergent field generated at all void tips with a small curvature. This divergent field distribution requires finer mesh size at these specific locations to ensure the accuracy of results. To address this, a local mesh refinement technique of figure 6 is introduced. The areas of field maxima are partitioned into spherical regions as shown.

This approach, leading to meshing illustrated in figure 7, also has the following advantages in both the mesh control and post-processes:

- subdivided domains allow the local refinement of mesh

- not only the minimum element size, but also the speed of mesh growth can be controlled inside the subdivided domain
- divided surfaces of the tree body allow not only local maxima but also integrated average electric fields to be determined conveniently
- sub-divided domains allow integrated volume electric field analysis

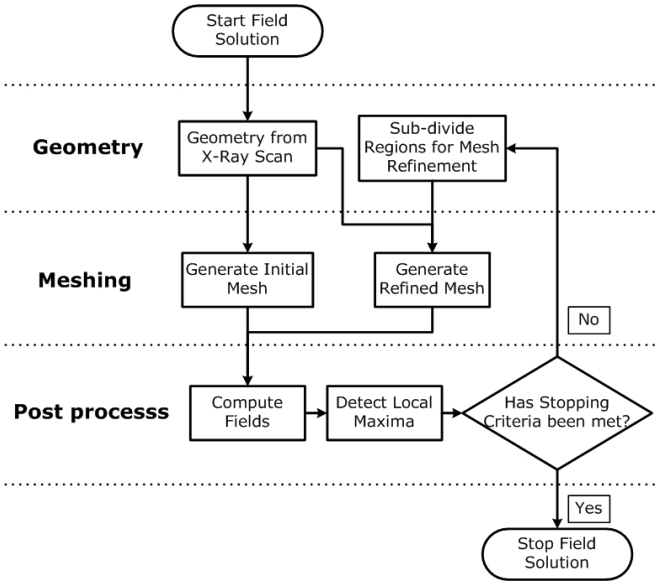

Figure 5. Mesh Scheme designed for Electrical Tree Modeling.

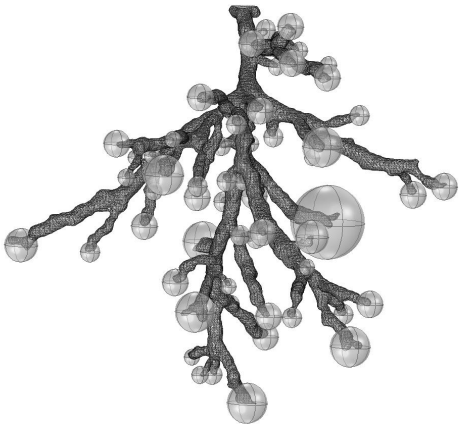

Figure 6. Regions of high field, segregated into spheres for refined meshing.

4.3 FEA ACCURACY

The previous section introduced an adaptive mesh scheme for refining the mesh. The stop criterion (in Figure 5) needs to be determined when the local mesh has been refined to an acceptable level. This section establishes a benchmark on how intense the mesh needs to be so that a certain level of accuracy can be achieved where the refinement loop shown in Figure 5 can be terminated.

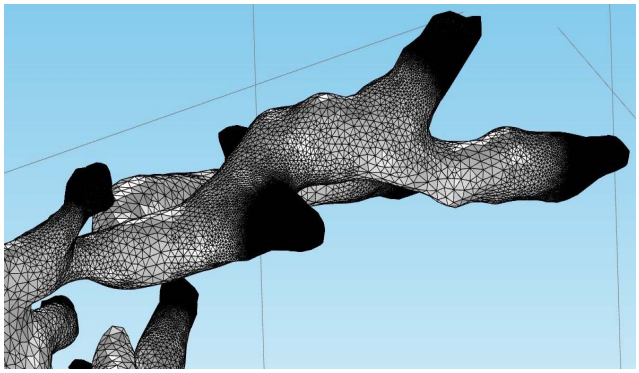

Figure 7. Higher mesh densities are used on the surfaces of small radii, as seen here at a branch tip.

A model of a sphere-plane gap, has been built to understand the equivalent errors which could exist in the tree model. This simplified model can be solved accurately by the Charge Simulation Method (CSM) and offers the opportunity to compare the FEA results with the analytical based method.

A perfectly conducting sphere above an infinite ground plane is shown in Figure 8. The sphere has a radius, R = 1μm and is placed at a distance 2 mm above the ground. The radius of this sphere simulates the smallest tips within electrical tree structure while the distance between the sphere and the ground reflects the distance between tree tips and the ground. The voltage applied is 18 kV. The space outside the sphere is filled with an insulation material with a relative permittivity of 3.6, representing the epoxy resin.

This model is first solved by CSM (programming in MATLAB). A series of fictitious point charges are constructed a distance below the surface of the sphere (the black points within Figure 8) to simulate the actual charge distribution on the sphere surface. Accuracy is determined by the number of point charges. The accuracy is evaluated by examining the deviation between the actual voltage on the sphere surface (18 kV) and that calculated from the fictitious point charges. It is found that the results stabilized at 18005 kV/mm when extra fictitious point charges only cause a deviation of less than 0.1% on the electric field. This value is then utilized as a benchmark against which to evaluate the accuracy of the finite element method.

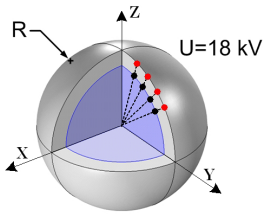

Figure 8. A sphere above an infinite ground plane. Used to verify the FEA results against the Charge Simulation Method.

As explained in the previous section, the accuracy of FEA relies on how the overall domain has been meshed. Finer mesh achieves higher accuracy but raises the computing power required. Moreover a mesh size smaller than the image resolution may provide a misleading confidence in the model accuracy which is fundamentally limited by the imported reconstruction. To examine the accuracy of the FEA electric field computation, various mesh sizes have been applied on this simplified sphere-to-ground model. As shown in Figure 9, the numerical residual reduced from 40% to below 1% when the mesh ratio τ (ratio between the minimum mesh size and the minimum curvature) is decreased from 0.5 to 0.05. If a ratio of 0.05 is preserved between the mesh size and original image resolution, the FEA error will be less than 1% and given the uncertainty in geometry, this will not be the limiting factor for the model accuracy.

As stated previously, such high fields are not expected in real materials, but this exercise shows the FEA meshing procedure adopted can provide spatial accuracy for features down to the 1 μm scale.

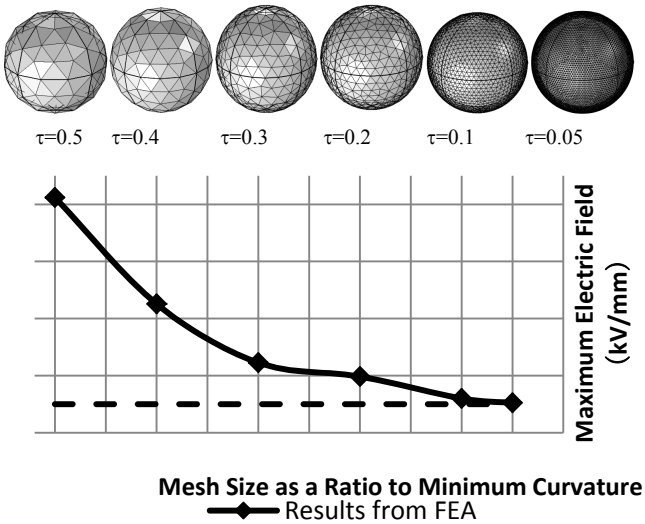

Figure 9. Maximum electric field predicted by FEA as a function of mesh size.

5 RESULTS AND ANALYSIS

In the nature of any numerical method, finite element methods seek for solutions to problems after reasonable simplifications have been made. By 'reasonable' is meant that the simplification is understood, quantified and only introduces errors in a known and acceptable manner. The development in computing resources has made the simulation of a geometry containing complex details (such as the tree model developed here) possible. Coupling different physics enables simulation of not only one physical parameter but also by other physical fields. With carefully designed simulation schemes, even nonlinear problems can be addressed with considerable accuracy. This section presents simulation strategies as well as their imposed limitations.

5.1 RESULTS FOR THE SIMPLIFIED MODELS

As discussed in Section 3, electrical trees can be classified as either:

- insulating (where the tree channels can be considered as air filled with no conductivity)
- conductive (conducting surface 10^{-3} Ωcm, and a wall thickness of 0.5 μm)
- conductive with extended ionization volume (conducting surface as above but only to within 100 μm of the tree tips)

To evaluate the sensitivity of various parameters, such as tree conductivity, wall thickness, and extended ionization volume, a simplified model (Figure 10) is introduced as a case study.

As shown in Figure 10, a needle with 3 μm tip radius is embedded in an epoxy cube (22 mm x 22 mm x 20 mm). A 60 μm long tree channel with a 3 μm tip radius extends from the tip of the needle. 18 kV is applied at the needle and the bottom surface of the epoxy cube 2 mm from the needle tip is grounded. To evaluate the effect of tree channel conductivity on the electric field distribution, a finite element model calculating the capacitive-resistive field is introduced. Within this model, the air has a relative permittivity of 1 and a conductivity of $1x10^{-15}$ S/m, the epoxy has a relative permittivity of 3.6 and a conductivity of $1x10^{-13}$ S/m. The tree channel has a relative permittivity of 1, but its conductivity varies depending on the nature of the tree (an insulating tree channel is given a homogeneous conductivity of $1x10^{-13}$ S/m while a conductive tree channel has a conductivity of $1x10^{-5}$ S/m).

A cut plane through the axis of rotational symmetry is introduced to present the 3D simulation results in 2D plots. The electric field distribution and potential contour are plotted in Figure 11a, b and c. The electric field drop along the tips of needle and tree channel are plotted in Figure 9d as a function of tree conductivity.

It is observed from the simulation results that:

- The highest electric field is located on the needle tip for an insulating tree channel
- The highest electric field is located on the tip of tree channel for a conductive tree channel
- In the two extreme case the fields are 2000 kV/mm as this is controlled by their radii which are the same in this model

One limitation of this model is that the conductivity of the dielectrics are not dependent on the local electric field strength and space charge is not considered. The 2000 kV/mm is then, whilst higher than expected in a real material, typical of an analytical calculation for a 3 μm conducting feature enhancing a Laplacian field [30, 31]. Incorporating field-dependent characteristics will be important in studying the mechanism of tree growth. FEA tools can readily accommodate non-linear field dependencies with iterative methods. This requires exponentially increased computing power (both processors and memories) and imposes a limitation on the complexity of model which could be resolved. Moreover it requires accurate knowledge of localized high field conductivities.

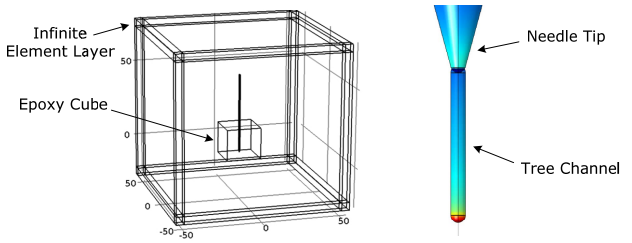

Figure 10. Geometry of complete model (left) and close-up of needle tip with a 3 µm radius (right).

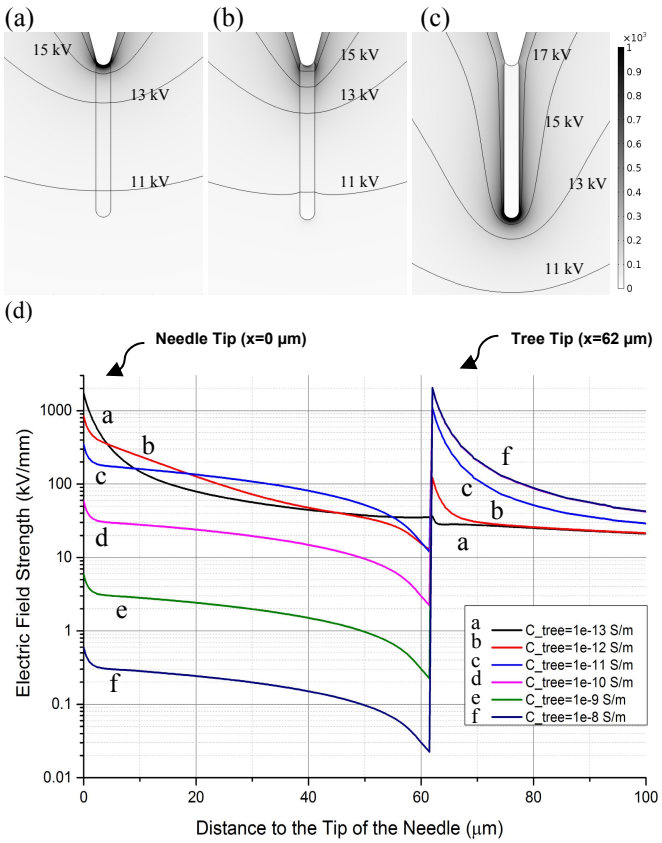

Figure 11. Electric field distribution and voltage contour for: (a) insulating tree (C_{tree}=10^{-13} S/m), (b) semi-conductive tree (C_{tree}=10^{-7} S/m) and (c) conductive tree (C_{tree}=10^{-5} S/m); (d) the electric field value against the distance along the line of symmetry through the needle tip.

5.2 RESULTS FOR BIFERCATING TREE CHANNELS

When a conductive tree starts to grow, it is likely to grow from the location where electric field is highest, such as the tip of a tree channel. At some stage a mother channel bifurcates into daughter channels. This newly developed geometry modifies the local electric field dramatically. To understand the mechanism of the procedure of tree growth, a good understanding of the electric field distribution is required. This section analyzes how FEA can assist in determining the magnitude and direction of the electric field strength as modified by a formative branched geometry.

A conductive tree channel (with the conductivity of 10^{-5} S/m) as described in the previous section is considered. The calculation of electric field takes into consideration of capacitive-resistive field. At the tip of the cylindrical tree channel, it is assumed that the main tree channel (mother) divided into two sub-channels (daughter branches) as shown in Figure 12. It is also assumed that one of the daughter branches follows exactly the same direction of the mother branch, the other daughter branch grows off at a certain angle: a typical angle of 60 degrees is considered here. The electric field distribution in both 3D and 2D are compared between a single channel and pronged channels, in Figure 12.

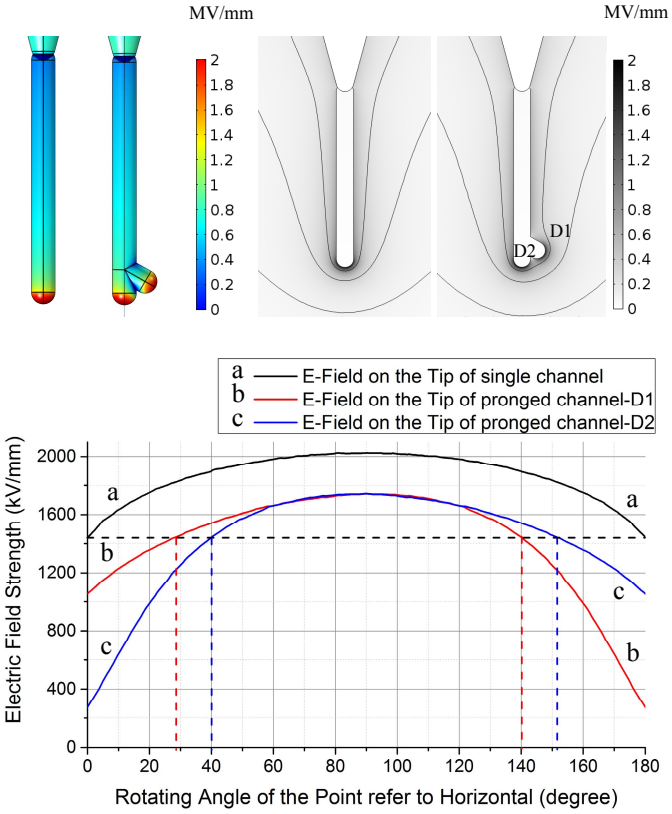

Figure 12. Regions of high field as a single channel starts to bifurcate.

From the results, it is observed that:

- From the single channel to the pronged channels, the magnitude of the maximum electric field is reduced 10%
- Due to the effect of the daughter branch, the direction of the maximum electric field shifted 6 degrees from the axis of rotation of the needle
- If the lowest electric field around the tip of a single channel is defined as a threshold value for tree growth. The area of the tip surface which could grow (has an electric field strength higher than the threshold value) on a pronged tree channels is reduced from 0-180 degree to 40-152 degree (as marked in dash line in Figure 12)

5.3 RESULTS FOR XCT MODEL

After the local mesh refinement, the electric field distribution surrounding the tree may be computed. The electric field is highest at tree tips where a divergent field is generated. The local maxima value is not only depending on the accuracy of X-ray scan but also on the numerical approximation when CAD tools are used to process geometries. Within this part of data analysis, the average and

maximum value of both the spherical surfaces and the volume domains surrounding tips are presented.

5.3.1 LOCAL MAXIMA AND AVERAGES AROUND TIPS

To describe the electric field strength at tree tips, local maxima and averages are considered. Local maxima refer to the highest electric field value within the 3D volume surrounding of a tip. The local average value is obtained by integrating the electric field within a 1 μm sphere of the maximum location – including only the solid region (i.e. not the air/branch space). This typically includes 100,000 voxels and so removes issues over errors associated with spatial resolution.

Figure 13 shows the locations of some of the branch tips (for clarity, not all are identified), and Figure 14 gives values of the local fields for all the 56 branch tips of the tree.

It is found that the highest average field is located at the furthest extent of the tree, closest to the ground plane; the highest maximum field is located at the sub-branch which is oriented at 45 degrees towards the bottom and left hand side. The lowest maximum and average is located a third of the way up the tree, shielded within the tree structure.

5.3.2 ELECTRIC FIELD GRADIENT AROUND BRANCH TIPS

As discussed in the previous section, the physical mechanism of tree growth is likely to be not only dependent on the local maximum value, but also the gradient and divergence surrounding the maximum point. To consider this a spherical surface is constructed, with the centre of the sphere at the maximum electric field position. By increasing the radius, the average electric field on the surface of the sphere may be detected. Here the radius of the sphere increased from 0.1 μm to 2 μm with 0.1 μm steps. T40 shown in Figure 13 is selected as an example to analyze both the field drop and direction of highest electric field. Figure 15 shows that from 0.1 to 2 μm, the electric field falls from 9000 kV/mm to 1200 kV/mm.

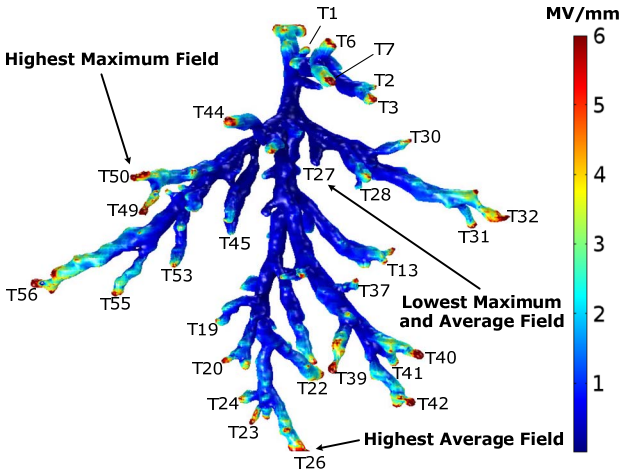

Figure 13. The locations of the maximum and minimum fields. To provide a representative view colours are scaled up to 6 MV/mm, all fields above that value are red. Peak values are given in Figure 14.

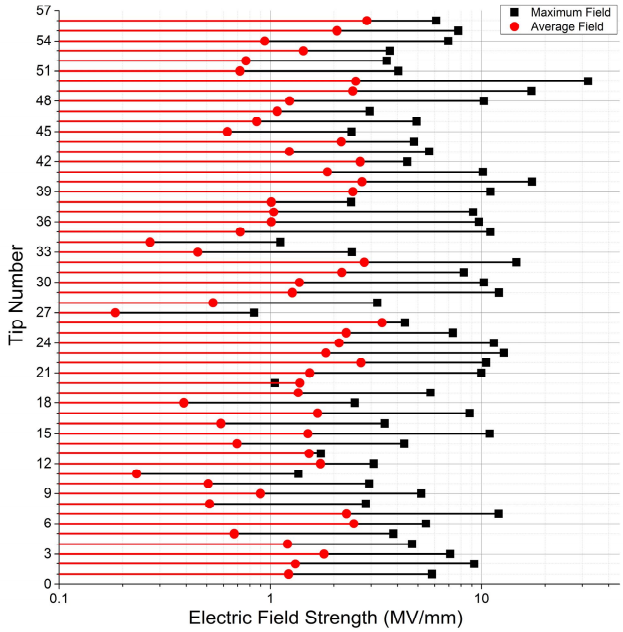

Figure 14. The average and maximum field determined for each conductive branch tip.

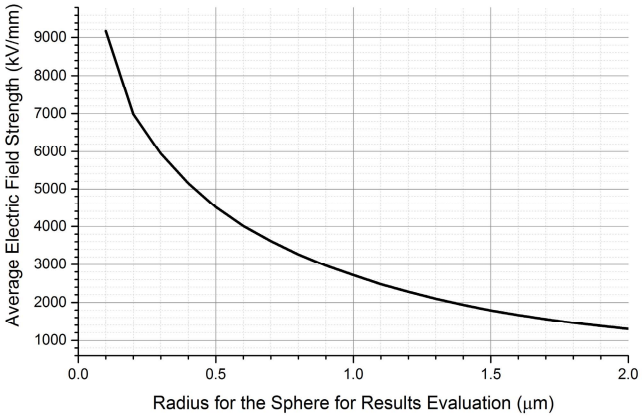

Figure 15. The average electric field drop over all tips plotted against the radius of sphere used for obtaining surface average value.

As the ionization process happens around tree tips, the distribution of electric field around tree tips is a critical parameter to determine in which direction the electrical tree will grow. The disadvantage of the approach of figure 13 is that the uncertainties and roughness of the surfaces impact the results. As an alternative approach, Figure 16 shows the electric field distribution around some tree tips on the equipotential surface at 90% of the energization voltage. A typical tip, T40, is selected to analyze the field distribution around the tree tips. This approach provides a smooth reproducible surface within the solid dielectric for analysis.

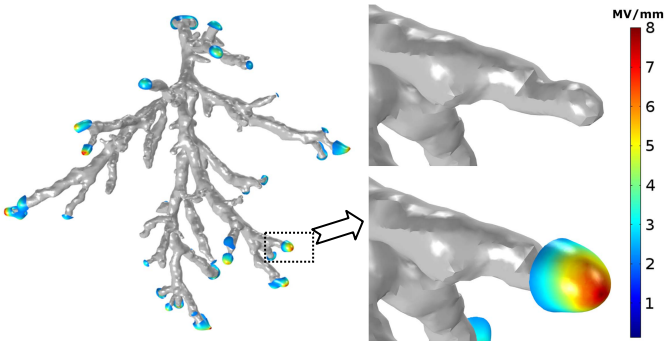

Figure 16. The electric field distribution over a tree tip surface. The tip labelled T40 in Figure 14 is arbitrarily chosen for the close-up view.

6 CONCLUSIONS

FEA has been shown to be a powerful tool with which to determine electric field distributions in and around electrical trees. FEA's limitations do not arise from the meshing capabilities if the models are correctly constructed. Methods have been shown to yield highly accurate results in simplified cases.

Two key factors do limit the applicability of this tool: Firstly the uncertainties surrounding real tree geometries. The 3D reconstructions generated using XCT and SBFSEM techniques provide excellent models for the larger features of the trees, above a micrometre. However the surfaces and smaller features are not distinct. Other techniques such as SEM and TEM may be used to determine more structural detail, and used in concert with the 3D approaches, however care is required so that preparation techniques do not alter the nature of the surfaces examined. Two techniques have been presented to overcome these issues, and use the generation of surfaces close to the tree surface, firstly using a geometric spherical construction around a tree tip, and secondly using equipotential surfaces.

The second factor which requires further study are the material properties used in the FEA models. Measurements for surface conductivity values are available for carbonised surfaces, but high field conductivity values are also required for the solid dielectrics. Moreover space charge in the gas and solid phases needs better understanding for inclusion in a comprehensive and realistic model.

An illustration has been provided suggesting FEA can be used to predict fields (magnitude and directions) for a complex tree. This suggests these may be used to predict and model tree development and growth, including topologies. Certainly a powerful platform has been developed for testing hypothesis concerning mechanisms of field-driven tree growth.

The model built has required assumptions concerning the physical properties of all materials concerned. In particular the surfaces of the tree tubules are likely to have a major effect on the discharge process through photo-ionization, recombination and space charge effects . As the process of discharge is not being considered here this has not been considered. For simplicity the models presented here have assumed a conducting tree, which removes many of the unknown parameters. Even so the dielectric properties of the polymer in the high field region at the tree tips are essential for a more realistic model. If less conducting trees are considered, is clear that the assumption of a non-conducting gas is unlikely to be satisfactory and this also needs further consideration.

ACKNOWLEDGMENT

This work is part of the EPSRC Supergen HubNet Project EP/I013636/1, http://www.hubnet.org.uk/. Roger Schurch would like to acknowledge the scholarship support of CONICYT (Chilean Research Council).

REFERENCES

[1] J. Mason, "The deterioration and breakdown of dielectrics resulting from internal discharges," Proc. IEE, Vol. 98, pp. 44–89, 1951.

[2] X. Chen, Y. Xu, X. Cao, S. J. Dodd and L. A. Dissado, "Effect of tree channel conductivity on electrical tree shape and breakdown in XLPE cable insulation samples", IEEE Trans. Dielectr. Electr. Insul., Vol. 18, pp. 847–860, 2011.

[3] N. Shimizu and C. Laurent, "Electrical tree initiation", IEEE Trans. Dielectr. Electr. Insul., Vol. 5, pp. 651-659, 1998

[4] R. M. Eichhorn, "Treeing in solid extruded electrical insulation", IEEE Trans. Electr. Insul., Vol. 12, pp. 2-18, 1977.

[5] L. A. Dissado and J. C. Fothergill, *Electrical Degradation and Breakdown in Polymers*. Peter Peregrinus for IEE, London, UK, 1992.

[6] L. Niemeyer, L. Pietronero and H. J. Wiesmann, "Fractal dimension of dielectric breakdown", Phys. Rev. Letters, Vol. 52, No. 12, pp. 1033-1036, 1984.

[7] K. Kudo "Fractal analysis of electrical trees", IEEE Trans. Dielectr. Electr. Insul., Vol. 5, pp. 713-727, 1998.

[8] A. L. Barclay, P. J. Sweeney, L. A. Dissado and G. Stevens, "Stochastic modelling of electrical treeing: fractal and statistical characteristics", J. Phys. D: Appl. Phys., Vol. 23, No. 12, pp. 1536-1545, 1990.

[9] X. Chen, Y. Xu, X. Cao, S. J. Dodd and L. A. Dissado, "Effect of tree channel conductivity on electrical tree shape and breakdown in XLPE cable insulation samples", IEEE Trans. Dielectr. Electr. Insul., Vol. 18, pp. 847–860, 2011.

[10] J. V. Champion, "The effect of material composition and temperature on electrical tree growth in epoxy resins", IET Conf. Dielectr. Materials, Measurements and Applications, Edinburgh, UK, pp. 30–34, 2000.

[11] B. X. Du, Z. L. Ma, Y. Gao and T. Han, "Effect of ambient temperature on electrical treeing characteristics in silicone rubber", IEEE Trans. Dielectr. Electr. Insul., Vol. 18, pp. 401-407, 2011.

[12] H.-Z. Ding and B. R. Varlow, "Thermodynamic model for electrical tree propagation kinetics in combined electrical and mechanical stresses", IEEE Trans. Dielectr. Electr. Insul., Vol. 12, pp. 81-89, 2005.

[13] N. Hozumi, T. Okamoto and H. Fukagawa, "TEM observation of electrical tree paths and micro-structures in polyethylene", Japanese J. Appl. Phys., Vol. 27, pp. 1230-1233, 1988.

[14] A. S. Vaughan, I. L. Hosier, S. J. Dodd, and S. J. Sutton, "On the structure and chemistry of electrical trees in polyethylene", J. Phys. D. Appl. Phys., Vol. 39, No. 5, pp. 962–978, 2006.

[15] R. Schurch, S. M. Rowland, R. S. Bradley, and P. J. Withers, "Imaging and Analysis Techniques for Electrical Trees using X-ray Computed Tomography", IEEE Trans. Dielectr. Electr. Insul., Vol. 21, pp. 53–63, 2014.

[16] R. Schurch, S. M. Rowland, R. S. Bradley, and P. J. Withers, "Comparison and Combination of Imaging Techniques for Three Dimensional Analysis of Electrical Trees", IEEE Trans. Dielectr. Electr. Insul., Vol. 22, No. 2, pp. 709-719, 2015.

[17] H. Uehara and K. Kudo, "Three-Dimensional Fractal Analysis of Real Electrical Trees in Polyethylene", Jap. J. App. Phys., Vol. 38, pp. 3604-3610, 1999.

[18] R. Schurch, S. M. Rowland, R. S. Bradley, T. Hashimoto, G. E. Thompson and P. J. Withers, "Three dimensional imaging of electrical trees in micro and nano-filled epoxy resin", IEEE Conf. Electr. Insul. Dielectr. Phenomena (CEIDP), Des Moines, Iowa, USA, pp. 39-42 2014.

[19] A. C. Kak and M. Slaney, *Principles of Computerized Tomographic Imaging*: Society for Industrial and Applied Mathematics, 2001.

[20] R. Fitzgerald, "Phase-Sensitive X-ray Imaging," Phys. Today, Vol. 53, pp. 23-26, 2000.

[21] W. Denk and H. Horstmann, "Serial block-face scanning electron microscopy to reconstruct three-dimensional tissue nanostructure", PLOS Biology, Vol. 2, pp. 1900-1909, 2004.

[22] J. C. Dainty and R. Shaw, *Image Science: Principles, Analysis and Evaluation of Photographic-type Imaging Processes,* Academic Press Inc., 1974.
[23] R. Schurch, S. M. Rowland, R. S. Bradley, and P. J. Withers, "Three dimensional characterisation of electrical trees", IEEE Conf. Electr. Insul. Dielectr. Phenomena (CEIDP), Shenzhen, China, pp. 494-497, 2013.
[24] A. C. Gjaerde and J. Sletbak, "Influence of partial discharges on void gas pressure", Int'l. Conf. Partial Discharges, Canterbury, UK, pp. 119–120, 1993.
[25] C. Mayoux and C. Laurent, "Contribution of partial discharges to electrical breakdown of solid insulating materials," IEEE Trans. Dielectr. Electr. Insul., Vol. 2, pp. 641–652, 1995
[26] A. S. Vaughan, S. J. Dodd, and S. J. Sutton, "A Raman microprobe study of electrical treeing in polyethylene," J. Mater. Sci., Vol. 39, No. 1, pp. 181–191, 2004.
[27] J. Champion and S. Dodd, "Simulation of partial discharges in conducting and non-conducting electrical tree structures," J. Phys. D. Appl. Phys., Vol. 34, pp 1235-1242, 2001.
[28] A. S. Vaughan, I. L. Hosier, S. J. Dodd, and S. J. Sutton, "On the structure and chemistry of electrical trees in polyethylene," J. Phys. D. Appl. Phys., Vol. 39, No. 5, pp. 962–978, 2006.
[29] L. A. Dissado, "Understanding electrical trees in solids: From experiment to theory", IEEE Trans. Dielectr. Electr. Insul., Vol. 9, pp. 483-497, 2002.
[30] R. W. Hare and R. M. Hill, "Space charge in insulators with needle-plane geometry", J. Phys. D. Appl. Phys., Vol. 24, pp. 398-406, 1991.
[31] L. Cisse, S. S. Bamji and A. T. Bulinski, "Electric field calculations for needle-plane geometry and space charge in polyethylene", IEEE Trans. Dielectr. Electr. Insul., Vol. 10 , pp. 176-180, 2003.

Simon M. Rowland (SM'07) was born in London, England. He completed the B.Sc. degree in physics at The University of East Anglia and the Ph.D. degree at London University. He has worked for many years on dielectrics and their applications and has also been Operations and Technical Director within multinational manufacturing companies. He joined The School of Electrical and Electronic Engineering in The University of Manchester as a Senior Lecturer in 2003, and was appointed Professor of Electrical Materials in 2009. He was President of the IEEE Dielectric and Electrical Insulation Society from 2011-12. He is an Associate Editor of the IEEE Transactions on Dielectrics and Electrical Insulation.

Roger Schurch (S'11) was born in Temuco, Chile. He received a degree in electrical engineering in 2006 from Federico Santa Maria Technical University (UTFSM), Valparaiso, Chile. He was a high voltage equipment analyst at Transelec transmission company in Santiago, Chile, during 2006-08. He joined the Department of Electrical Engineering UTFSM, as a Junior Lecturer in 2008, where he also carried out dielectric tests for mining and utility companies. Since 2011, he has been a Ph.D. degree student at the School of Electrical and Electronic Engineering in The University of Manchester. His research project involves the study of electrical trees and partial discharges in polymeric insulation. He was awarded a IEEE Graduate Fellowship of the Dielectrics and Electric Insulation Society in 2011.

Michalis Pattouras was born in Nicosia, Cyprus. He received the M.Eng. degree in electrical and electronic engineering at The University of Manchester in 2011. Since then, he has been a Ph.D. degree student at the School of Electrical and Electronic Engineering in The University of Manchester. His research project involves the understanding of the role of material interfaces (joints) on failure processes in HV equipment. He is studying electrical tree behavior across interfaces and ways to inhibit this phenomenon.

Qi Li (aka Steven) was born in Hunan Province, China, in September 1984. He completed the B.Eng. degree in electrical and electronics engineering at both the University of Birmingham and Huazhong University of Science and Technology, in 2007 (as an exchange student). He received the M.Sc. degree with distinction in electrical power engineering from the University of Manchester in 2009, and completed the Ph.D. degree in the same institution in 2013. Dr Qi Li is currently working as a research assistant in the National Grid High Voltage Research Centre in the University of Manchester, UK. His main research interests include: surface potential gradient calculation for overhead line conductors, the mechanism of hum noise from transmission lines and audible noise evaluation for different types of conductors.